

TESTS ON AN AC LIQUID-METAL CONDUCTION MACHINE

Yu. A. Bakanov, L. G. Vlasenko,
S. E. Dvorchik, Ya. Ya. Zandart,
V. K. Makarevich, V. E. Strizhak,
I. M. Tolmach, and S. R. Troitskii

UDC 621.313.3:538.4

The design and construction are presented for a high-temperature form of ac conduction machine. Test results are given for a sodium loop in the generator and pump modes. An oscillogram is presented for the self-excitation of the device. A method has been developed for calculating the expected parameters of the machine at high pressures on the basis of tests obtained at small pressure differences.

Features of ac Conduction Machines

A model for a high-temperature conduction liquid-metal machine was drawn up, made, and tested in 1970 to compare theory with experiment and to evaluate design features for such devices.

The following are among the advantages of ac conduction machines: 1) there is no restriction on the working voltage such as occurs in dc conduction machines; 2) the winding and magnetic system are comparatively simple, there being none of the slots usual in induction machines, and it is possible to increase the induction in the gap; 3) there are only small end losses on account of the large ratio of channel length to width (8-15); 4) there is no transverse edge effect such as occurs in three-phase induction machines.

The main disadvantages of these machines are the difficulties in soldering the primary turn to the channel and in providing strength in this part of the design, as well as the presence of eddy losses proportional to the cube of the channel width.

This last feature is responsible, among others, for the low efficiency of previously designed conduction pumps for ac, since the working velocities have been small, only 2-5 m/sec. However, if one chooses higher speeds of 20-50 m/sec, the width of the channel becomes substantially less, and the eddy losses can be reduced to less than 5% of the useful power input.

Theoretical System and General Design

Figure 1 shows the general design of the machine; the windings 1 carry ac, so the magnetic circuit 6 produces in the zone of the working channel 3 an alternating field. The direction of liquid metal flow in the four channels is shown by the crosses and the points in the circles in the figure. All the channels were of outside cross-section $16.6 \times 6.4 \text{ mm}^2$ with an active length of 250 mm and a wall thickness of 0.5 mm (Kh18N10T steel); these were soldered together and to the primary copper turn 5 of the transformer with hard solder. The emf arising in each channel on motion of the liquid metal will be in series, on account of the primary current in the transformer I_1 .

The core 4 of the transformer takes the usual W form; the secondary winding 2 consists of two sections, which are placed on the end rods of the core and are joined in series.

The machine can work as an independently excited generator, a generator with self-excitation, and a pump. Figure 1 shows the connection circuit for windings 1 and 2, the working load R_L , and the capacitor

Translated from *Magnitnaya Gidrodinamika*, No. 2, pp. 124-129, April-June, 1973. Original article submitted April 27, 1972.

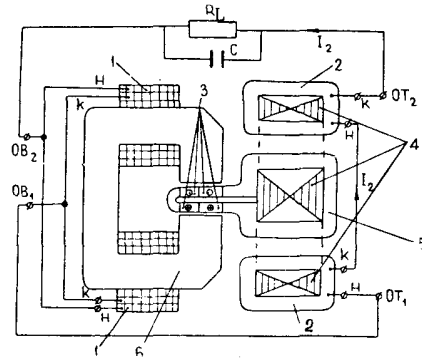


Fig. 1

Fig. 1. Theoretical system.

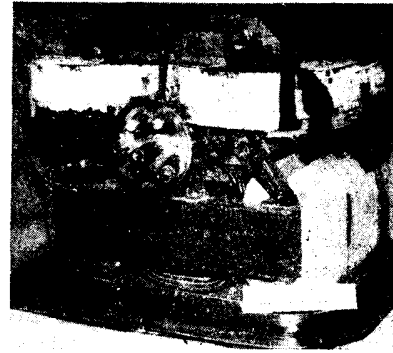


Fig. 2

Fig. 2. General view of the experimental model with the cover removed.

C for a self-excited state. This circuit is a self-excited oscillatory one. The energy in this state enters from the moving liquid metal and passes to the primary turn 5, then to the winding 2, and then is consumed in the loss in winding 1 and the useful power supplied with resistance R_L .

In the pump mode, the external supplies go to the excitation winding 1 and the secondary winding 2 of the transformer, and the phase shift between the currents in these windings is important. The largest pressure effect is produced when the two currents are in phase, i.e., when the windings are joined in series. Figure 2 gives a general view of the machine with the cover removed.

The material for the magnetic circuit is made of a cobalt alloy known as Permendur, which has a Curie point of about 900°C . The sheets of magnetic material 0.2 mm thick are insulated one from another by heat-resisting material 3-5 μm thick. Special heat-resisting materials are used to insulate the windings.

The thin-walled channels are strengthened in the active zone by the flat surfaces of the pole tips, which are insulated with thin layers of mica. The inlet and outlet zones in the channel are lacquered with heat-resisting material. The entire system can work up to 600°C . To protect the heated elements from corrosion and contact with air the machine has an outer jacket, within which there flows argon. The electrical leads are brought out through the jacket via seals based on ceramic and covar. The machine also includes turns for measuring the magnetic flux, the thermocouples, and two tapoffs for liquid metal.

Figure 3 shows the hydraulic circuit of the machine in the sodium loop, which contains two pumps 4, which can produce together pressure up to 25 kgf/cm^2 , an electromagnetic flow meter 3, the pressure gauges M2, M9, and M3, which measure the inlet, outlet, and intermediate pressures, the cooler 1, and the differential gauge 2.

An additional feature of the four-channel model is the need for parallel hydraulic connection of the channels, with countercurrent flow in each pair (Fig. 3). This leads to electrical loops in the conducting tubes $\text{OPRR}_1\text{S}_1\text{O}$ and $\text{O}_1\text{P}_1\text{R}_1\text{SO}_1$, which link with part of the alternating excitation flux (points R and R_1 have electrical contact via the body of the machine).

To suppress the currents arising in these loops, with their resulting losses, we introduce the compensating magnetic circuits K_1 and K_2 , which are connected in series with the excitation winding. The numbers of turns on the coils were selected by experiment in order to suppress the current in the loops, which was monitored by means of suitable terminals.

Basic Relationships.

Here we give without deduction the basic relationships for the machine in the self-excited generator mode, as used in design:

$$\Delta p - \Delta p_f (V) = I_1^2 (\alpha + \beta V), \quad (1)$$

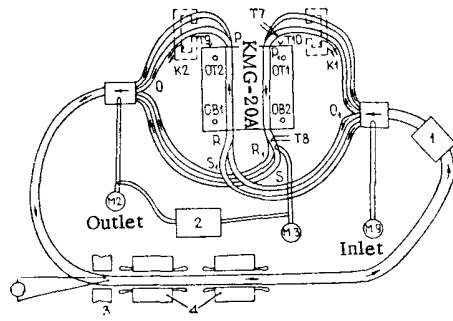


Fig. 3

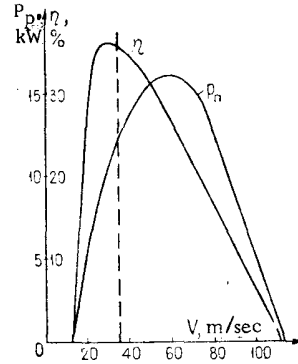


Fig. 4

Fig. 3. Hydraulic scheme for the loop.

Fig. 4. Design characteristics in the generator mode ($\Delta p = 30 \text{ kgf/cm}^2$).



Fig. 5. Self-excitation as a generator (voltage scale 1 mm = 100 V, time scale 1 mm = 0.008 sec).

where

$$\alpha = \frac{C_B}{\gamma \Delta}; \quad \beta = \frac{\sigma C_B}{\gamma} \left[\left(\gamma - 1 + \gamma \frac{m^2}{1+2m} \right) l + \frac{h K_1^2}{\pi \gamma} C_1 \right]. \quad (2)$$

Here Δp is the total pressure drop on one channel, which is provided by the external pressure source, $p_f(V)$ is the pressure drop in the channel due to friction without the magnetic field for the same flow speed, I_1 is the current going to the channel electrode (effective value), V is the mean (flow) speed in the channel, and C_B is the coefficient of proportionality between the current and the effective value of the induction in the gas:

$$B = C_B I_1. \quad (3)$$

Note that strictly speaking B is proportional only to the excitation current I_2 . Since the currents I_1 and I_2 are closely related to the primary and secondary currents of the transformer, which have only a small magnetizing current, we therefore have (3). The quantity

$$\gamma = 1 + 2\sigma_1 \Delta_1 / \sigma \Delta,$$

where σ and σ_1 are the electrical conductivities of the working body and the material of the channel wall; Δ and Δ_1 are the gaps in one channel for the liquid metal and the thickness of one wall of the channel; l is the active length of one channel; m is the power law for the velocity profile in the channel (in the depth direction), which is assumed distributed in this way; h is the width of one channel; $K_1 \approx 0.8$ is the ratio of the voltage on the electrodes to the emf from the motion; C_1 is a coefficient less than 1 that defines the reduction in the end loss on account of the special measures taken, such as the fall in the field at the ends of the channel, introduction of insulating baffles, and so on.

We multiply both parts of (1) by $4G$, the flow rate in the channels, to get the energy relationship

$$P_h = P_m + P_e, \quad (4)$$

where $P_h = \Delta p \cdot 4G$ is the total hydraulic loss, $P_m = \Delta p_f(V) \cdot 4G$ is the loss due to viscous friction, and $P_e = I_1^2 (\alpha + \beta V) \cdot 4G$ is the electrical power.

TABLE 1

Flow rate, liters/sec	Experiment							Calc.	
	pressure, kgf/cm ²			T, °C	f, Hz	Δp, kgf/cm ²	Δp _f , kgf/cm ²	P _n , W	P _n , W
	M-9	M-2	M-3						
11,2	11,42	2,72	3,2	305	17	7,74	6,2	368	350
11,8	11,42	2,8	3,28	305	17	7,64	6,8	263	227
11,25	11,85	2,68	3,16	305	17,5	8,21	6,25	487	460
11,15	12,1	2,68	3,12	305	17,5	8,54	6,1	465	550
11,15	12,4	2,72	3,16	305	17,5	8,73	6,1	495	590

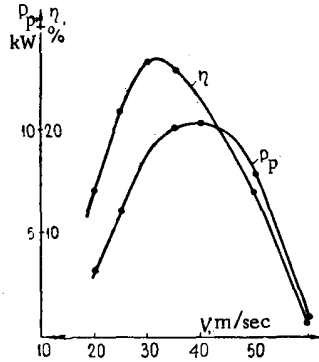


Fig. 6. Characteristics of machine as a generator with heavy loading.

In turn,

$$P_e = P_{e1} + P_J + P_p + P_c \quad (5)$$

where $P_J = (I_1^2 \sigma C_B / \gamma)(\gamma - 1) l V \cdot 4G$ is the Joule loss in the walls of the channel, while $P_p = [I_1^2 \sigma C_B m^2 / (1 + 2m)] l V \cdot 4G$ is the Joule loss arising from the nonuniformity of the velocity profile, with $P_e = (I_1^2 \sigma C_B K_1^2 / \pi \gamma^2) G \cdot 4C_1 V$ the end losses and $P_{e1} = (C_B / \gamma \Delta) I_1^2 \cdot 4G$ the part of the electrical power transmitted to the primary turn of the transformer.

The useful power P_p is equal to P_{e1} less the Joule loss in the entire primary turn (including the channels) due to the through current I_1 , as well as less any Joule loss in the secondary winding and in the excitation winding, together with the eddy current loss P_B in the liquid metal passing through the excitation winding and the loss in the steel in the insulated magnetic circuits.

From this with (3) and $G = \Delta h V$ we get

$$P_p = \frac{4h C_B I_1^2 V}{\gamma} - I_1^2 \left(\Sigma r + \frac{4h}{\gamma \sigma \Delta l} \right) - P_B - P_{st} \quad (6)$$

Here Σr is the sum of the resistances for the copper in the primary winding and the relative resistance of the secondary winding and excitation winding as referred to the primary circuit.

We assume as a first approximation that P_B and P_{st} are proportional to the square of B , and thence to the square of I_1 :

$$P_B + P_{st} = C_2 I_1^2 \quad (7)$$

Then we may write for the useful power that

$$P_p = I_1^2 (\beta_1 V - \alpha_1) \quad (8)$$

where

$$\beta_1 = \frac{4h C_B}{\gamma}; \quad \alpha_1 = \left(\Sigma r + \frac{4h}{\gamma \sigma \Delta l} \right) + C_2 \quad (9)$$

It follows from (1) and (8) also that

$$P_p = \frac{[\Delta p - \Delta p_f(V)] (\beta_1 V - \alpha_1)}{\alpha + \beta V} \quad (10)$$

Equation (10) is suitable for a check calculation on the machine in the generator mode; one specifies definite dimensions, and then finds α , β , α_1 , and β_1 . For the given external pressure difference Δp we determine P_p as a function of V . The efficiency of the machine in the generator mode is found from

$$\eta = P_p / 4 \Delta p G \quad (11)$$

Figure 4 shows the design characteristics of the machine as calculated from (10) and (11) for the following initial parameters: working body, potassium at 550°C; temperature of whole machine, 500°C; $\Delta p = 30$ kgf/cm²; optimal mode (shown in Fig. 4 by the broken line); efficiency 36%; useful power 12.4 kW; flow rate 11.8 kg/sec; and frequency 30 Hz.

EXPERIMENTAL RESULTS

All tests showed that the design was essentially viable when the system with the intermediate transformer was used with self-excitation; a pressure difference of 8 kgf/cm² was used with a flow rate to all the channels of 8.8 kg/sec, with the machine and the sodium at 300°C, which gave a useful output of 500 W and an efficiency of 5.5% with an oscillation frequency of 18 Hz. Other modes of operation provided less power. The machine showed good self-excitation even without preliminary charging of the capacitor (Fig. 5).

In the pump mode, the useful pressure difference was 1.3 kgf/cm², with a sodium flow rate of 2.8 kg/sec and an efficiency of 5% at 300°C and 50 Hz. The total time for hot working was 44 h. Increase in pressure to over 8 kgf/cm² and operation at a nominal pressure of 31 kgf/cm² was not possible, since a leak arose in one of the channels. Subsequent demounting showed that the leak arose in the middle part of the channel, at the edge as a result of a latent defect in the tube that was revealed by the elevated pressure.

Equations (10) and (11) enable one to predict the expected power and efficiency from results obtained at low pressure differences. The parameters α , α_1 , β , and β_1 were derived from experiments, as was $\Delta p_f(V)$, which substantially increased the reliability of the calculation. The data processing was as follows. From the open-circuit characteristic derived from 25 runs we found C_B is $0.328 \times 10^{-4} \Omega \text{ sec/m}^2$.

Comparison with the design value showed that the induction in the working volume was about 8% less than the design value in the generator mode, which was probably due to the demagnetizing action of the current in the liquid metal on account of incomplete compensation. We found α_1 from the results for several generator runs; the values ranged from $40.4 \cdot 10^{-6}$ to $45.9 \cdot 10^{-6} \Omega$ in three runs at 18 Hz.

On the other hand, the α_1 calculated from (9) using the design parameters and all the technological elements was $32 \cdot 10^{-6} \Omega$. The likely explanation of this discrepancy is that the sodium incompletely wets the internal surface of the channel. For instance, we found that at 8 h after starting to pump the sodium through the channels, conduction effects were still absent, i.e., there was no wetting at $\alpha_1 = \infty$. Wetting set in only after 24 h of pumping, but it was then not complete. One expects that α_1 would approach the above $32 \cdot 10^{-6} \Omega$ when wetting was complete.

The other parameters were $\sigma = 5.95 \cdot 10^{-6} \text{ mho} \cdot \text{m}^{-1}$; $\sigma_1 = 1.09 \cdot 10^6 \text{ mho} \cdot \text{m}^{-1}$; $\Delta = 6 \text{ mm}$; $\Delta_1 = 0.5 \text{ mm}$; $\gamma = 1.0305$; $m = 0.07$ (assumed); $l = 25 \text{ cm}$; $K_1 = 0.8$ from (2) and (9), and $\alpha = 5.32 \cdot 10^{-3}$; $\beta = 61.2 \cdot 10^{-6}$; $\beta_1 = 19.9 \cdot 10^{-7}$.

Flushing of the channels with sodium in the absence of a magnetic field gave the resistance coefficient as about 0.026, which represented the usual level.

Figure 6 gives the calculation of P_p and η for $\Delta p = 31 \text{ kgf/cm}^2$ with the above values of the parameters derived from experiment. One therefore expects from the machine a useful output of 9.6 kW and an efficiency of 27% at $V = 32 \text{ m/sec}$ ($4G = 12 \text{ liters/sec}$) and a temperature of 300°C.

The verification of the calculation of (10) is provided by Table 1, which relates to several self-excited generator runs and provides comparison with calculations based on the above parameters.

Comparison of the last two vertical columns indicates satisfactory agreement.

Figure 6 indicates an efficiency of 27% at a power of about 10 kW, so we can say from the design studies that one should attain an efficiency of 40% at 100 kW and 50% at 500 kW. This increase in efficiency is of scale origin.